REPORT DOCUMENTATION PAGE

Form Approved
OMB No. 0704-01-0188

The public reporting burden for this collection of information is estimated to average 1 hour per response, including the time for reviewing instructions, searching existing data sources, gathering and maintaining the data needed, and completing and reviewing the collection of information. Send comments regarding this burden estimate or any other aspect of this collection of information, including suggestions for reducing the burden to Department of Defense, Washington Headquarters Services Directorate for Information Operations and Reports (0704-0188), 1215 Jefferson Davis Highway, Suite 1204, Arlington VA 22202-4302. Respondents should be aware that notwithstanding any other provision of law, no person shall be subject to any penalty for failing to comply with a collection of information if it does not display a currently valid OMB control number.
PLEASE DO NOT RETURN YOUR FORM TO THE ABOVE ADDRESS.

DTIC COPY

1. REPORT DATE *(DD-MM-YYYY)*
04-08-2007

2. REPORT TYPE
REPRINT

3. DATES COVERED *(From - To)*

4. TITLE AND SUBTITLE
Electron attachment to SF_6 under well defined conditions: Comparison of statistical modeling results to experiments

5a. CONTRACT NUMBER

5b. GRANT NUMBER

5c. PROGRAM ELEMENT NUMBER
61102F

5d. PROJECT NUMBER
2303

5e. TASK NUMBER
BM

5f. WORK UNIT NUMBER
A1

6. AUTHORS
Thomas M. Miller*, Albert A. Viggiano, and Jurgen Troe**

7. PERFORMING ORGANIZATION NAME(S) AND ADDRESS(ES)
Air Force Research Laboratory/RVBXT
29 Randolph Road
Hanscom AFB, MA 01731-3010

8. PERFORMING ORGANIZATION REPORT NUMBER
AFRL-RV-HA-TR-2008-1143

9. SPONSORING/MONITORING AGENCY NAME(S) AND ADDRESS(ES)

10. SPONSOR/MONITOR'S ACRONYM(S)
AFRL/RVBXT

11. SPONSOR/MONITOR'S REPORT NUMBER(S)

12. DISTRIBUTION/AVAILABILITY STATEMENT
Approved for Public Release; distribution unlimited.

13. SUPPLEMENTARY NOTES
Reprinted from: Journal of Physics: Conference Series **115** (2008) 012019, doi:10.1088/1742-6596/115/1/012019, © 2008 IOP Publishing Ltd.
*Boston College, Chestnut Hill, MA 02467 *Univ. of Gottingen, Tammanstrasse 6, D-37077 Gottingen, Germany

14. ABSTRACT
Experiments were carried out using a flowing-afterglow Langmuir-probe apparatus to measure rate constants for electron attachment to SF_6 and thermal detachment from SF_6^-. In a recent series of papers, these results were combined with new and existing data on nondissociative and dissociative attachment to SF_6 and compared to statistical modeling of the various processes involved in the stabilization of the ionic products of attachment. This paper gives a summary of those findings. The major conclusions are: (a) only the ground electronic state of SF_6 needs to be invoked to explain available data; (b) the electron affinity of SF_6 is higher than previously thought, namely, $EA(SF_6 = 1.20 (\pm 0.05)$ eV; (c) the endothermicity of the dissociative electron attachment reaction that yields SF_5^- is 0.41 eV ($\pm$ 0.05) eV at 0 K; (d) combining these two numbers gives the bond energy $D_0°(F—SF_5^-) = 1.61 (\pm 0.05)$ eV.

15. SUBJECT TERMS
Electron attachment Sulfur hexafluoride Statistical theory Rate constants

16. SECURITY CLASSIFICATION OF:			17. LIMITATION OF ABSTRACT	18. NUMBER OF PAGES	19a. NAME OF RESPONSIBLE PERSON
a. REPORT	b. ABSTRACT	c. THIS PAGE			Albert Viggiano
UNCL	UNCL	UNCL	UNL	13	19B. TELEPHONE NUMBER *(Include area code)*

AFRL-RV-HA-TR-2008-1143

15th International Symposium on Electron Molecule Collisions and Swarms IOP Publishing
Journal of Physics: Conference Series **115** (2008) 012019 doi:10.1088/1742-6596/115/1/012019

DTIC COPY

Electron attachment to SF_6 under well defined conditions: Comparison of statistical modeling results to experiments

Thomas M. Miller[1], Albert A. Viggiano[1], and Jürgen Troe[2]

[1] *Air Force Research Laboratory, Space Vehicles Directorate, Hanscom Air Force Base, Bedford, Massachusetts 01731-3010, USA*

[2] Institute for Physical Chemistry, University of Göttingen, Tammannstrasse 6, D-37077 Göttingen, Germany

E-mail: miller.hanscom@gmail.com

Abstract. Experiments were carried out using a flowing-afterglow Langmuir-probe apparatus to measure rate constants for electron attachment to SF_6 and thermal detachment from SF_6^-. In a recent series of papers, these results were combined with new and existing data on nondissociative and dissociative attachment to SF_6 and compared to statistical modeling of the various processes involved in the stabilization of the ionic products of attachment. This paper gives a summary of those findings. The major conclusions are: (a) only the ground electronic state of SF_6^- needs to be invoked to explain available data; (b) the electron affinity of SF_6 is higher than previously thought, namely, $EA(SF_6) = 1.20 (\pm 0.05)$ eV; (c) the endothermicity of the dissociative electron attachment reaction that yields SF_5^- is 0.41 eV ($\pm$ 0.05) eV at 0 K; (d) combining these two numbers gives the bond energy $D_0^o(F—SF_5^-) = 1.61 (\pm 0.05)$ eV.

I. Introduction

In three earlier papers we delineated various aspects of electron attachment to SF_6 and the reverse detachment from SF_6^- under thermal and low-energy conditions (electron energies less than about 0.4 eV).[1-3] There exists also a wealth of information on the higher energy processes, but those are outside the scope of the present study. For a more detailed discussion of the higher-energy processes, see the reviews by Christophorou and Olthoff.[4,5] Our goal in the earlier papers was to present a complete and consistent picture of the numerous steps involved in the electron attachment reaction. This required new experimental and theoretical techniques. The flowing-afterglow Langmuir-probe apparatus (FALP) was used in new ways to make measurements on electron attachment and thermal detachment under truly thermal conditions over extended temperature and pressure ranges. In order to explain both the new and previous data, statistical theories that were developed for neutral and ion- molecule reactions were modified for use in understanding electron processes. The new measurements combined with the detailed modeling allowed derivation of the electron affinity of SF_6 and the bond energy $D_0^o(F—SF_5^-)$.

While the SF_6 system has been and continues to be the most studied electron attachment reaction, many aspects of the reactivity have appeared in conflict or remain unexplained. Due to the complexity of the system, the modeling presented in our earlier papers focused on the intricate detail needed to understand a wide range of experimental observations. In this paper, we will present the current understanding of the electron attachment reaction with SF_6, passing over the details of the

© 2008 IOP Publishing Ltd

20090213270

measurements and modeling. We are only focused on thermal or low-energy processes for both associative and dissociative attachment to SF_6 as well as thermal detachment from SF_6^-. The regime of interest is sometimes referred to as the zero-energy resonance. Higher energy resonances include formation of SF_4^-, SF_3^-, SF_2^-, F_2^-, and F^- and are not discussed. In addition, we focus on the most informative results and do not intend to give a comprehensive review—see Christophorou and Olthoff.[4,5]

Our earlier series of papers clearly showed the need for a complete characterization of the experimental conditions used in making measurements on this reaction, including the average electron energy, as well as the electron energy distribution, the temperature of SF_6, the number density and identity of the gas in the interaction region, and the transit time from the interaction region to the detector. Thermal measurements always have the conditions well defined, though not necessarily specified in publications. In contrast, beam experiments can be difficult to interpret unless all parameters are not only well defined but accounted for in the data analysis. In order to present an overall, consistent picture of the reaction, we will discuss a number of pitfalls that can occur in measurements.

II. Production of SF_6^-

The overall reaction scheme is shown in figure 1. The first step in the reaction sequence is electron capture into a resonant continuum state, which we denote by e^-SF_6,

$$e^- + SF_6 \rightarrow e^-SF_6 \qquad \textit{capture.} \qquad (1)$$

The description of step (1) for SF_6 is provided by pure *s*-wave capture, which is commonly modeled by the formula due to Klots[6] which deviates by as much as 8% from the correct Vogt-Wannier *s*-wave cross section.[7] A new, more accurate formula for the *s*-wave capture cross section $\sigma_c(E)$ as a function of electron energy E has been presented by Dashevskaya et al.,[8]

$$\sigma_c(E) = (\pi/2E)[1 - 0.5\exp(-\sqrt{8\alpha E}) - 0.5\exp(-\sqrt{72\alpha E})] \qquad \textit{s-wave capture,} \qquad (2)$$

where α is the molecular average polarizability in a_o^3, E is the electron energy in hartree, and $\sigma_c(E)$ is in a_o^2. The new formula has deviations of <2% from the Vogt-Wannier *s*-wave capture cross section. Dashevskaya et al. also presented formulas for capture involving higher-order partial waves and ion-dipole interactions (not needed for low-energy attachment to SF_6).[8]

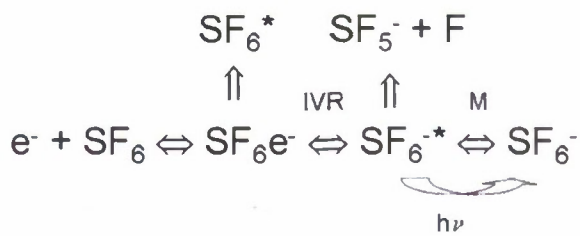

Figure 1. Scheme showing the individual processes involved in the electron-SF_6 reaction.

The nascent e^-SF_6 can then undergo intramolecular vibrational redistribution (IVR) to form highly vibrationally excited SF_6^{-*} in its ground electronic state, with the total energy still in the continuum,

$$e^-SF_6 \rightarrow SF_6^{-*} \qquad \textit{IVR.} \tag{3}$$

The reverse of process (3), followed by the reverse of process (1), is detachment

$$SF_6^{-*} \rightarrow e^-SF_6 \rightarrow e^- + SF_6 \qquad \textit{detachment.} \tag{4}$$

Additionally, electrons can vibrationally excite the neutral SF_6 (shown as SF_6* in figure 1)[7,9].

$$e^- + SF_6 \rightarrow e^-SF_6 \rightarrow SF_6^* + e \qquad \textit{vibrational excitation.} \tag{5}$$

In order to form stabilized SF_6^-, i.e., with a total energy below the continuum, energy needs to be dissipated from SF_6^{-*} through radiation

$$SF_6^{-*} \rightarrow SF_6^- + h\nu \qquad \textit{radiative stabilization} \tag{6}$$

or through collisions with a third body,

$$SF_6^{-*} + M \rightarrow SF_6^- + M \qquad \textit{collisional stabilization.} \tag{7}$$

In addition, a dissociative channel, yielding SF_5^- + F, can open up. That process will be discussed in the next section.

Each process listed above is important in determining cross sections and rate constants for SF_6^- production in some pressure, temperature, or energy regime. In our earlier papers, the modeling of each step was presented, either through statistical theory or from calibration to experimental data.[1-3] In particular, detachment, IVR, and vibrational excitation cross sections are difficult to calculate from first principles, so the relevant parameters were determined from measured cross sections or rate constants. Likewise, the radiative contribution, equation (6), was calibrated using ion-cyclotron resonance (ICR) measurements of the stabilization of SF_6^{-*} at very low pressures. A master equation governing energy gain and loss in collisions was used to model collisional stabilization [equation (7)], with parameters determined from ion-molecule reaction studies.

The first set of experimental data discussed here are rate constants as a function of temperature for the overall attachment process in the high pressure limit. There is general agreement on the 300 K rate constants with many groups finding values near the very accurate measurements of Crompton and coworkers,[10,11] and for this reason, relative cross section measurements taken as a function of electron energy are usually normalized to the Crompton value of $2.27 \pm 0.07 \times 10^{-7}$ cm^3 s^{-1} at 295 K. Crompton and coworkers also measured a rate constant of $2.20 \pm 0.09 \times 10^{-7}$ cm^3 s^{-1} at 500 K, indicating that there is little temperature dependence, and imperceptible difference between buffer gases, in their pressure range of 8-23 Torr. However, low temperature measurements carried out with the CRESU (Cinétique de Réaction en Ecoulement Supersonique Uniforme) technique[12] showed an unexpected temperature dependence. Figure 2 shows the complete temperature range of available data along with the s-wave capture curve. The rate constants from 48-173 K lie well below the canonical room temperature value. In particular, from 48 to 123 K, rate constants were found to be independent of temperature at about 60% of the Crompton et al. values. From 123 to 300 K, the measured rate constants increased. It should be noted that T_{el} in the CRESU experiment was later found to range from T_{gas} up as high as 500 K due to superelastic collisions between electrons and vibrationally-excited N_2 buffer gas.[13] This contamination is not thought to affect CRESU results for SF_6 for T_{gas} in the 48-123 K range, at least, because the measured attachment rate constants appear independent of T_{gas}. New results in the temperature range 300-670 K from our laboratory were presented in our earlier series of papers[1,3], and show good agreement with Crompton et al. in the overlapping region and begin to fall slightly above 550 K, to a value of 2.0×10^{-7} cm^3 s^{-1} at 670 K. Many older measurements are cataloged in the reviews by Christophorou and Olthoff,[4,5] which show that the

attachment rate constant falls continuously for temperatures above 700 K. The temperature data along with electron temperature data, and modeling results are plotted in Figure 3 as a function of electron temperature. The modeling results include all steps outlined in equations 1, 3-7. The model well represents the data for electron attachment to SF_6 in the high-pressure limit.

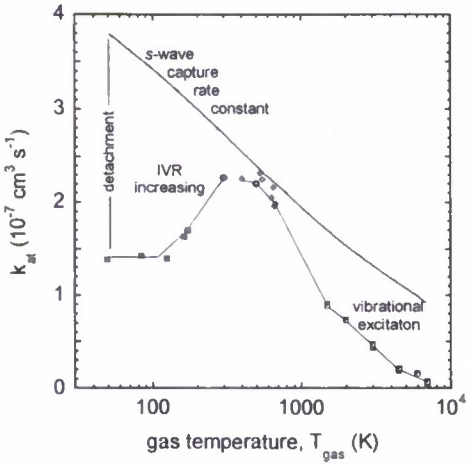

Figure 2. Total rate constants for electron attachment to SF_6, in the high-pressure limit, versus gas temperature. The departure from the *s*-wave capture rate constant provides input for modeling, as indicated (roughly) by the labeling. The data from 48-300 K are from Ref. 12. Those from 300-670 K are the present FALP data, except for the large dark circles (Refs. 10 and 11). Data at high electron temperature from ORNL are used to indicate trends expected for high T_{gas} (Refs. 4 and 5).

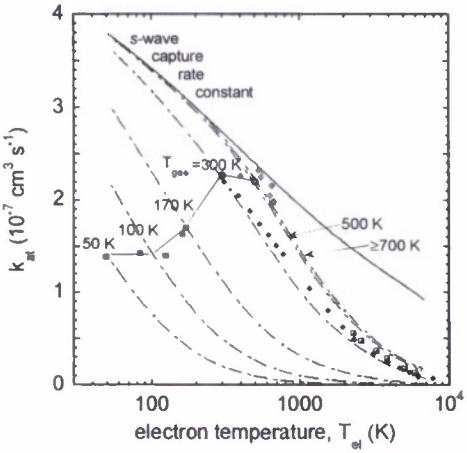

Figure 3. Predicted total rate constants for electron attachment to SF_6, in the high-pressure limit, versus electron temperature, for the fixed gas temperatures indicated by labels. The data shown are the same as in Fig. 2 except for those showing the T_{el} dependence (♦ for T_{gas} = 300 K as recommended in Refs. 4 and 5, and ◘ for T_{gas} = 500 K from Ref. 13).

Modeling the thermal attachment rate constants by averaging the Vogt-Wannier cross sections of equation (2) over a Boltzmann distribution of electron energies E leads to larger values than measured. This discrepancy at low temperatures is attributed to incomplete IVR where this process competes with autodetachment. Initially, the IVR reduction factor was modeled by a value that was independent of gas temperature. This proved inadequate to fit the temperature dependence shown in figure 2. Instead, it was necessary to have the IVR rate increase with increasing temperature, i.e., dependent upon the degree of vibrational excitation of the SF_6 molecule. The *s*-wave rate constant decreases monotonically with temperature, but the attachment rate constant increases mainly because the IVR efficiency increases. The rate constant eventually comes close to the *s*-wave collisional value, then decreases faster than the collisional rate constant with temperature, as more electron collisions go to vibrational excitation without attachment. The experimentally fitted IVR probability, with coefficients varying with temperature, were given in equation (3.6) and Table 3 of Ref. 1. At high

temperatures, the discrepancy between modeled capture rate constants and experimental data is attributed to the competition between attachment and vibrational excitation, equation (5). Tentatively, the corresponding reduction factor was taken independent of temperature.

The modeling of the various processes versus electron energy allowed us to predict how the attachment rate constants would change for electron temperature (T_{el}) different from the gas temperature (T_{gas}). These results are shown in figure 3 along with data from the Oak Ridge National Laboratory (ORNL) recommended in Ref. 4, for T_{gas} = 300 K, and ORNL data from Ref. 14 for T_{gas} = 500 K.

III. Pressure Dependence

The discussion immediately above dealt exclusively with the high pressure limit of the reaction. A complete understanding, and therefore a faithful modeling of the rate constants, must also include pressure dependences. Much of the literature acknowledges that stabilization must be included in the attachment mechanism but then ignores the stabilization step in the interpretation of results, based on the general agreement of experimental data obtained in buffer gas pressures from 1 Torr to several atm. In the absence of radiative stabilization, the attachment rate constants should increase linearly with pressure (low pressure limit), then increase at a rate slower than pressure (falloff region), and finally saturate so that further increases in pressure do nothing (high pressure limit). Radiative stabilization is evident in the ICR data of Foster and Beauchamp.[15] At 300 K, they found that the attachment rate constant was 1.6 (± 0.2) × 10^{-8} cm^3 s^{-1}, independent of SF_6 pressure below 5 × 10^{-7} Torr. The long observation time (20-80 ms) in the ICR enabled those measurements to be made. The low pressure rate constant is only 7% of the value measured at high pressures. As N_2 gas was added to the cell, the attachment rate constant increased as expected, reaching 4.8 × 10^{-8} cm^3 s^{-1} at 7.3 × 10^{-5} Torr N_2.

The pressure dependence can be represented using the master equation approach of statistical theory, as formulated in Ref. 1 for the SF_6 problem. The master equation describes the effect of collisions on SF_6^{-*}, in competition with autodetachment, radiative stabilization, and dissociation (into SF_5^- + F). Collisions with buffer gas may increase or decrease the internal energy of SF_6^{-*}, but there is a net decrease, on average. The modeling requires knowledge of this average decrease in internal energy. A value of 200 cm^{-1} for a N_2 buffer gas was used, based on modeling of unimolecular decomposition of vibrationally excited ions.[16] Expressions for the pressure dependence were given as equations (6.1) and (6.2) in Ref. 1. The resulting falloff curves are shown in figure 4 (dashed lines) for an N_2 buffer gas at a variety of temperatures. The effect of radiative stabilization is shown by the solid curves in figure 4, based on modeling of the Foster and Beauchamp[15] ICR data at 300 K, yielding a radiative rate constant of 53 s^{-1}. An analysis based on *ab initio* calculations of radiative rates for vibrational states gave a value of 80 s^{-1},[17] in very good agreement with the modeled value. The model results are given in figure 4 and show that at low temperatures attachment rate constants approach the high pressure limit already at buffer gas concentrations corresponding to mTorr pressures. By 700 K, nearly 1 atm of N_2 is required to place an experiment in the high pressure limit. For a 300 K target gas, the radiative limit is reached only at concentrations below about 10^{-6} Torr.

Literature data show no apparent influence on the type of buffer gas used in experiments,[4,11] which is understandable in that almost all data to date have been obtained in or near the high pressure limit. If additional ICR data could be obtained at μTorr pressures, it is expected that differences could be observed, because the average energy ⟨E⟩ transferred per collision in the master equation describing collisional relaxation will be different for different gases. Beam data in the lowest energy regime simulate the high pressure limit since the lifetime for autodetachment is greater than the observation window. As the energy increases this is no longer true, and the data not only reflect the fundamental process being studied but also the instrument time window.

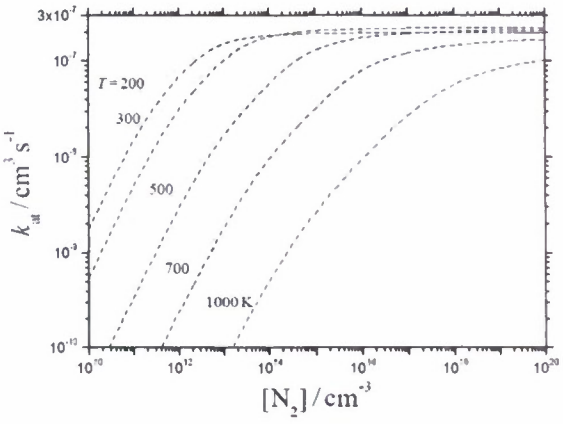

Figure 4. Predicted pressure dependence of rate constants for electron attachment to SF_6 for various gas temperatures. The solid curves include radiative stabilization of the SF_6^{-*}

IV. SF_5^- Production

SF_5^- may be produced following the initial attachment event in a slightly endothermic process.

$$SF_6^{-*} \rightarrow SF_5^- + F \qquad \textit{dissociation.} \qquad (8)$$

The SF_5^- branching fraction must be dependent on pressure since there is competition between SF_6^{-*} undergoing detachment, collisional and radiative stabilization, and dissociation. Previously, only the Fehsenfeld,[18] Foster and Beauchamp,[15] Crompton and Haddad,[10] and Petrović and Crompton[11] studies mentioned looking for a pressure dependence, aside from work conducted at very high pressures.[4,5] The pressure range in the Fehsenfeld experiment was 0.2-1.5 Torr (He gas) and 0.1-0.4 Torr (Ar gas) and no significant change was seen in either the rate constants or branching fraction.[18] The Australian experiments were carried out over a pressure range of 8-23 Torr of N_2, CO_2, H_2, and He.[10,11] Measurements at ORNL (see Christophorou and Olthoff[4,5]) have been carried out between 1-16 atm of N_2, Ar, and Xe, and earlier drift tube work in that laboratory utilized a wide variety of molecular gases at atm pressure and higher. As discussed above, the low pressure ICR study found the overall rate constant to rise with pressure. When one combines the Fehsenfeld[18] and ICR[15,19] values for the SF_5^- fraction, one sees a distinct pressure dependence. At essentially zero pressure in an ICR study, 5% SF_5^- is observed but at 1 Torr only ~0.01% is observed.

Španěl et al.[20] in 1995 noted the large difference in the SF_5^- branching fraction between Fehsenfeld's experiment at 1 Torr and the very low pressure experiment of Chen and Chantry.[21] They showed that the difference was due to collisional stabilization at 1 Torr gas pressure. From an analysis using RRK theory (see Refs. 20 and 22), they derived an endothermicity of 0.12 eV for the production of SF_5^-. The statistical modeling of the present work yields a larger value for the endothermicity. The more advanced nature of the recent statistical modeling yields a bond strength of $D_0^\circ(F\text{-}SF_5^-) = 1.61$ (± 0.05) eV.[2] The latter figure, combined with an improved electron affinity, $EA(SF_6) = 1.20$ (± 0.05) eV (Sect. VI) gives an endothermicity of 0.41 eV (at 298 K) for appearance of the SF_5^- product in the electron attachment reaction.

Modeling results for the specific rate constants for autodetachment [equation (3)] and dissociation [equation (8)] are shown in figure 5. The curves start from the respective thresholds and increase dramatically with energy. Once energetically possible, dissociation quickly dominates, i.e., at

energies <0.1 eV above threshold. To a large extent the vastly different slopes are a result of the fact that detachment is an s-wave-only phenomenon and therefore does not have multiple J states involved. Dissociation includes all partial waves.

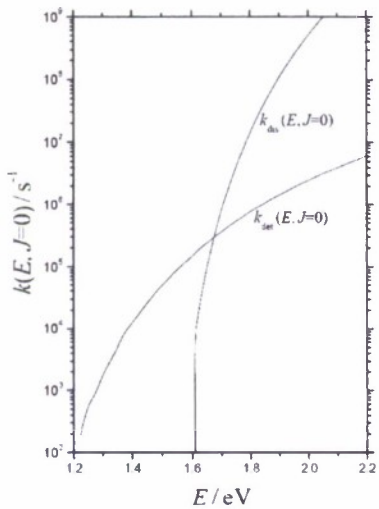

Figure 5. Specific rate constants for electron detachment of SF_6^{-*}, $k_{det}(E,J=0)$, and for dissociation to $SF_5^- + F$, $k_{dis}(E,J=0)$.

While the pressure dependence is rarely studied, the temperature and electron energy dependencies for SF_5^- production have long been recognized. In fact, the first mention of increase in SF_5^- fraction with higher temperature came already in 1958.[23] The temperature dependence is strikingly large. However, in order to compare the amount of SF_5^- formed in various experiments, it is important to look not only to the temperature and energy in an experiment, but also whether the SF_6^{-*} has had time to dissociate. The dissociation process will go to completion only in the presence of sufficient three-body collisions (to complete the stabilization of those SF_6^{-*} which haven't dissociated) or with a long observation window such as found in the ICR experiments. A long time window would allow radiative stabilization to come to an end and is therefore in the 0.1 s or longer range (several half-lives). Therefore, determining meaningful SF_5^- branching fractions in beam experiments is problematic. The observation window is typically 100 μs, but lifetimes for SF_6^{-*} can reach into the tens of ms.

We have addressed the previous scarcity of data on pressure dependences in two ways. Experimentally, we measured branching fractions as a function of pressure at multiple high temperatures where appreciable dependences were expected in the pressure range accessible in the FALP. We also confirmed the 1 Torr temperature dependence of branching fractions, as observed by Fehsenfeld at lower temperatures[18]. In addition, statistical modeling of the dependences were carried out with adjustable parameters fixed to a small subset of the data. Modeling results were given for the fraction of SF_5^- ion product as functions of gas temperature, electron temperature, and pressure, including collision-free conditions, in figures 6, 7, 9, and 10 of Part II of the earlier series of papers.[2]

Here we show in figure 6 modeling results for the SF_5^- branching ratio as a function of pressure at various high temperatures, for $T_{el} = T_{gas}$. Our experimental results agree well in the range where thermal detachment (see Sect. V) does not interfere; for simplicity, those data are not shown (see figure 3 of Ref. 2). As expected, temperature and pressure work in opposite ways for SF_5^- production. Increasing pressure increases the fraction of SF_6^- through stabilization of the excited intermediate, and increasing temperature increases the SF_5^- yield since the dissociation rate increases dramatically with internal energy of the SF_6^-. Examining the data, one finds pressure increases in importance with increasing temperature. This is because an increase in the internal energy of SF_6

reduces the lifetime of SF_6^{-*}, which in turn causes the reaction to move further from the high pressure limit into the falloff region. Experiments in the mTorr region would be informative but unfortunately are not available. At temperatures of 560 K and above, the branching data were found to depend on the residence time in the FALP, due to thermal reactivation of stable SF_6^- and subsequent detachment, i.e., thermal detachment. No other ion products other than SF_5^- and SF_6^- were observed at temperatures up to 670 K.

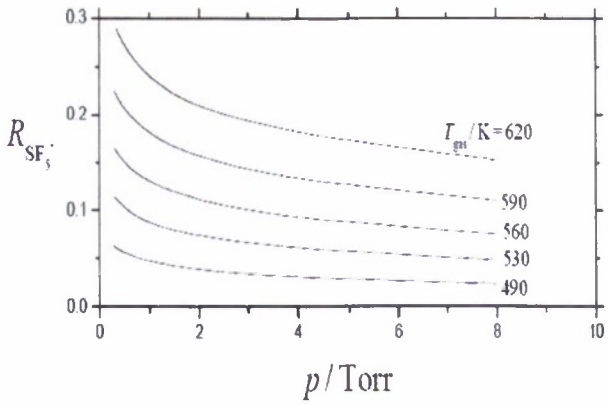

Figure 6. Model results for SF_5^- branching fractions for dissociative attachment under collision-free conditions.

One particularly interesting aspect of the data is that at 590 K the branching fraction reaches the high pressure limit and that significant quantities of SF_5^- are still produced, i.e., typical Stern-Volmer behavior is not followed. Modeling by a simple stepladder analysis, which involves only collisions that reduce the energy of SF_6^{-*}, cannot account for this behavior. Instead, we were forced to use the more accurate and time consuming master equation method, which allows for both energy increasing (up) and energy decreasing (down) collisions. Without the inclusion of up collisions, all SF_6^{-*} would eventually be quenched and no SF_5^- would be observed at high pressure. The up collisions included in the master equation lead to SF_6^{-*} ions with enough energy to dissociate rapidly, i.e., before stabilization can occur in a second collision.

One outcome of this analysis is to confirm an observation made by Španěl et al.[20] and verified by Smith et al.[24] that the peak in the SF_5^- signal observed in beam experiments around an electron energy of 0.3 – 0.6 eV is due to enhanced dissociation of SF_6^{-*} as a result of vibrational excitation by the incoming electron. Our model of this effect was shown in figure 11 of the earlier Part II paper,[2] for collision-free conditions, with a comparison to data by Braun et al.[25] Figure 7 shows measured and modeled cross sections for SF_5^- production as a function of electron energy. The two-peak nature of the data is well reproduced by the ground state only model. The decrease at low energy essentially follows the SF_6^- yield and results exclusively from vibrationally excited SF_6 thermally populated. The increase observed at 0.1 eV is the result of the steep dependence of k_{dis} on energy shown in figure 5. The data peak when essentially all products are SF_5^- and decrease according to the total cross section decrease.

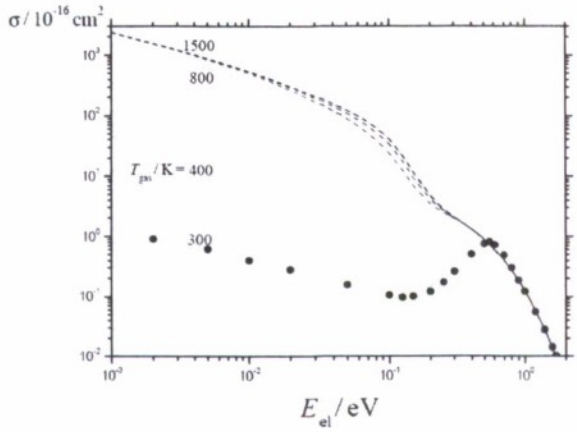

Figure 7. Total (---) and dissociative (——) cross sections as a function of T_{gas} and E_{el} (lines = modeling from this work for T_{gas} as indicated, see text; points = experimental data from Ref. 25 for T_{gas} = 300 K.

V. Autodetachment and Thermal Detachment

Hidden in the above discussion has been the importance of detachment processes at high temperatures. Branching fraction data obtained at high temperature with the FALP showed the importance of thermal detachment. In this process, energy is transferred to stable SF_6^- in collisions with the buffer gas. The SF_6^{-*} that is formed has enough energy to detach the electron,

$$SF_6^- + M \rightarrow SF_6^{-*} + M \qquad \textit{thermal activation.} \qquad (9)$$

Since dissociation occurs at substantially higher energies than detachment, and the SF_6^{-*} is formed near threshold, thermal detachment dominates over thermal dissociation, and the latter is not discussed further. Champion et al.[26] have shown that at higher energies dissociation becomes significant, as indicated by the relative k(E,J) curves for detachment and dissociation. Thermal detachment has been mainly ignored previously although it was looked for at temperatures below 600 K and not observed (see Christophorou and Olthoff[4] and Španěl et al.[20]) In order to determine thermal detachment rates, the SF_6^-/SF_5^- ratio at fixed temperature, pressure, electron concentration, and SF_6 concentration was measured as a function of residence time in the FALP apparatus. Since this ratio is extremely sensitive to detachment, rate constants on the order of tens of s^{-1} could be accurately determined. Above 560 K, a detachment rate constant was measurable. SF_6^- detachment rate constants of 22 (590 K), 40 (620 K), 114 (650 K), and 166 s^{-1} (670 K) were measured. Combining the detachment and attachment rate constants measured under the exact conditions allows for determination of the electron affinity $EA(SF_6)$, as discussed in the following section.

VI. Thermodynamics

There are two important thermodynamic quantities needed in the calculations and the new data allow for accurate determinations of both the electron affinity of SF_6 and the bond dissociation energy $D_0^o(F—SF_5^-)$. Recent reviews of these quantities are found in Christophorou and Olthoff,[5] Miller et. al.[27] and Lobring et al.[28] $EA(SF_6)$ has a long history of being difficult to measure in spite of numerous efforts. This is in part due to the large bond length change in going from SF_6 to SF_6^-, though both have octahedral symmetry. Therefore, the Franck Condon overlap is poor, and finding the origin band

corresponding to the EA, in photoelectron spectra, is difficult if not impossible.[29] Similarly the competition between SF_5^- and e^- production makes the determination of the bond energy difficult experimentally.

In the present study, we have measured rate constants for both attachment and detachment under exactly the same conditions. Combining these yields the the equilibrium constant,

$$e^- + SF_6 \Leftrightarrow SF_6^-;\ K = k_{at}/k_{det} \qquad \textit{equilibrium.} \qquad (10)$$

From the equilibrium constants and calculated frequencies for SF_6 and SF_6^-, by a third-law analysis the electron affinity is found to be 1.20 (± 0.05) eV.[2] There have been numerous previous determinations of the electron affinity with no general consistency in the values. A recent review[5] lists two similar values as the preferred choice[30,31] but one of those is from interpretations[31] known to have problems (see Ref. 32). Therefore, the charge transfer equilibrium value[30] of 1.05 (± 0.10) eV has been considered the established value. The present value for $EA(SF_6)$ is 0.15 eV larger than this, just at the limits of the combined uncertainties. Our data do not seem compatible with the lower value. A value $EA(SF_6)$ = 1.05 eV would lead to detachment rate constants 15 times larger than the measured ones at 650 K, which would have resulted in quite obvious upcurving of FALP electron density decay plots, with detachment overwhelming diffusive loss of electrons. While the FALP determination of $EA(SF_6)$ is based mainly on the ratio of k_{at} to k_{det}, it also involves adjustments due to the entropy and heat capacity changes in going from anion to neutral SF_6. The detachment rate constant k_{det} may be written as[33]

$$k_{det} = k_{at} N_A (273.15/T) \exp[-(EA/kT)-(\Delta S^\circ/k)-(H_T-H_0)/kT]. \qquad (12)$$

In equation (2), k is Boltzmann's constant, N_A is the Avogadro constant, EA is the electron affinity (at 0 K, by definition), ΔS° is the entropy change due to electron attachment at temperature T, and H_T-H_0 is a thermal energy correction from the measurement temperature to 0 K. Equation (11) is written to emphasize that the thermal electron detachment rate constant is not solely a function of EA and T, but also depends on the entropy change at temperature T and on a heat capacity term. The adjustments are calculated based on neutral and anion symmetries, rotational constants and vibrational frequencies and, in other cases we have studied, affect EA from <1% to nearly 9%.[34] In the case of SF_6 the calculated adjustments amount to 0.1 eV or 9%, i.e., they are significant. This point is emphasized because the SF_6 anion frequencies are not as well established as are those for the neutral, and require a high-level calculation to achieve the desired accuracy; see Ref. 3.

The bond dissociation energy for SF_6^- is determined from a detailed fitting of the SF_5^-/SF_6^- ratio under well defined conditions, both thermal and those taken as function of electron energy. Only a narrow range of $D_{298}^\circ(F—SF_5^-)$ gives good fits to a variety of data. A value of 1.61 (± 0.05) eV reproduces the data well. Two recent values for this quantity are 1.32 eV by Španěl et al.[20] (adjusting by the new EA) and <1.85 eV by Lobring et al.[28] The former is derived from simple RRK modelling of the SF_5^- branching rates. The detailed modelling present here should supplant that. The latter is derived from threshold measurements of SF_5^- production in the collision induced dissociation of SF_6^-. The less-than sign was attributed to a barrier in the reaction, but may be due to a neglect of the collisional electron detachment channel. We find no barrier need be postulated, in agreement with Španěl et al.[20] Table 1 in Lobring et. al.[28] shows a variety of computational values for $D_0^\circ(F—SF_5^-)$. Values range from 1.51-1.60 eV from compound Gaussian methods, 1.52 eV from a coupled cluster calculation, and 1.01-2.11 eV from a study using density functional theory. Not included is a value of 1.65 eV from the compound G3 method.[27] All of these computational ranges are consistent with our determination of $D_0^\circ(F—SF_5^-)$ = 1.61 (± 0.05) eV.[2]

VII. Lifetimes

Lifetime measurements for SF_6^{-*} have been made over a number of years with poor agreement. For instance, the two most recent measurements are 19.1 μs and 1 to >10 ms (Refs. 35 and 36, respectively). Typically, beam experiments find short lifetimes and trap experiments long lifetimes that depend on storage time (see Liu et al.[36]). Our results address this discrepancy.

Lifetimes and $k_{det}(E,J)$ curves (see figure 5) are the inverse of each other (possibly including integration). Our results show that the lifetime will strongly depend not only on the total energy, E, but also the total angular momentum J. For instance at, $k_{det}(1.4\ eV, J = 0) \approx 10^4\ s^{-1}$ and $k_{det}(1.4\ eV, J = 100) = 60\ s^{-1}$. The latter is about the same at $k_{det}(1.25\ eV, J = 0)$. Obviously the exact formation mechanism matters greatly. For thermal processes, the $k_{det}(E,J)$ used in the present calculations are more consistent with the trap measurements. In this range, radiative stabilization can compete with detachment. Higher-energy SF_6^{-*} will dissociate faster leaving species with longer lifetimes. Both processes will tend to lead to lifetime measurements that increase with time as have been observed.

We postulate several ideas for the large disparity in lifetimes. The SF_6^{-*} formation process needs to be well defined so that the energy and angular momentum of the complex is well known. If any collisions take place after formation, the lifetime will change dramatically because of the steep energy dependence of the specific rate constant $k_{det}(E,J)$, see figure 5. They also have significant structure around threshold, as shown in figure 6 of our earlier paper,[1] so that the energy distribution of the electron source becomes an important consideration. Assuming lifetimes ~10 ms and a collisional value for the energy transfer rate constant ($\sim 10^{-9}\ cm^3\ s^{-1}$), one finds number densities as low as $\sim 10^{11}$ cm will alter the lifetime. An order of magnitude lower pressure still effects 10% of the SF_6^{-*} molecules. In supersonic beams with ill-defined SF_6 temperatures, lifetimes are effected by both E and J dependences. This results both from the $k_{det}(E,J)$ for detachment and for IVR since IVR increases with increasing temperature. The lack of IVR would leave the complex as e^-SF_6 rather than SF_6^{-*} which would decrease the lifetime. This may be an issue in the recent determination by Le Garrec et al.[35] A potential problem not discussed previously in lifetime measurements is that large electric fields can strip electrons off highly excited molecules. In zero electron kinetic energy (ZEKE) experiments this is a well known issue and electron detachment occurs even at energies slightly below threshold. Large extraction fields may then lead to shorter apparent lifetimes.

VIII. Remaining Issues

It is worth mentioning issues that are unresolved. First is the question of whether F^- should be observable in attachment to SF_6 with zero-energy electrons. G3 theory gives an endothermicity of 1.18 eV for this channel at 298 K.[27] The NIST WebBook gives data which place this channel at 0.55 eV endothermic, the difference being in a low value of $D(SF_5\text{-}F)$ used by NIST, a value which was reexamined by Tsang and Herron.[37] Their bond strength is consistent with the result of G3 calculations. Braun et al.[25] see a very weak F^- ion signal, 3-4 orders of magnitude lower than the SF_6^- signal. They left open the possibility that the F^- was due to impurities, and planned further work. Because of the report of Braun et al., we used the FALP to search for an F^- signal in attachment to SF_6 at 585 K, and place a limit of <0.02% for the branching fraction for F^- based on the width of our baseline. This limit includes a mass discrimination correction which was uncovered in recent FALP work.[38]

Earlier we referred to results on photoelectron spectroscopy of SF_6^-.[29] That work showed a resolved, long progression of vibrational excitation in the ν_1 symmetric stretch mode of SF_6 as a result of detachment of the extra electron. It also showed a companion peak which was unexplained until recently, as simultaneous excitation of ν_1 and ν_4 modes.[39] Reference 29 also contained infrared vibrational predissociation spectra for SF_6^-, in which a resolved ν_1 transition was observed. Those spectra also contained structure, which is unexplained as of this writing. Thus, not everything may be known about the vibrational structure of SF_6^-.

IX. Conclusions

Experimental studies were conducted on electron attachment to SF_6 and on thermal electron detachment from SF_6^- to provide input for statistical modeling of the extensive body of data on the electron-SF_6 reaction system at low electron energies. In particular, the pressure dependence of attachment and detachment were examined, because little attention has been paid to collisional stabilization in the past. The details of the modeling were presented in earlier papers.[1-3] Empirical rate constants for the various processes (figure 1) involved in the electron attachment and stabilization problem were used to predict temperature, pressure, and electron temperature dependence of the attachment and dissociation (into F + SF_5^-) processes. Most absolute electron attachment experiments carried out to date have been in the high-pressure limit, where collisional equilibration occurs between SF_6^- and SF_5^-. The present modeling shows that the high-pressure limit moves to higher pressures as the gas temperature is increased. Aside from the new attachment and detachment rate constants measured, the main conclusions which may be drawn from this work are (1) only the ground electronic state of SF_6^- need be invoked to explain available data; (2) the electron affinity of SF_6 is higher than previously thought – we find EA(SF_6) = 1.20 (± 0.05) eV; (3) the endothermicity of the dissociative electron attachment reaction that yields SF_5^- is 0.41 (± 0.05) eV at 0 K; (4) combining these two numbers gives the bond energy D_0°(F—SF_5^-) = 1.61 (± 0.05) eV.

The modeling of the specific rate constants of the competing processes is, of course, dependent upon the quality of the experimental data. While there are a number of experimental data sets that are in agreement on, for example, the attachment rate constant in the high-pressure limit, other vital data are the product of single reports. It would be most helpful if future experiments could be carried out to (a) pin down EA(SF_6) more accurately, (b) confirm the low temperature results of Ref. 12, (c) confirm the very low-pressure ICR work of Ref. 15 and provide pressure dependences for electron attachment in the μTorr to mTorr region, and (d) provide additional thermal electron detachment data for SF_6^-. We are hoping to be able to extend some of our own measurements to higher temperatures at some point in the future.

X. Acknowlegments

This research was funded by the United States Air Force Office of Scientific Research under Project 2303EP4. Encouragement of this work by M. Berman, helpful discussions with H. Hotop and E.E. Nikitin, technical assistance by A. I. Maergoiz, as well as support by the Deutsche Forschungsgemeinschaft (SFB 357 "Molekulare Mechanismen unimolekularer Prozesse") are gratefully acknowledged.

References

[1] Troe J, Miller T M and Viggiano A A 2007 *J. Chem. Phys.* **127** 244303.
[2] Troe J, Miller T M and Viggiano A A 2007 *J. Chem. Phys.* **127** 244304.
[3] Viggiano A A, Miller T M, Friedman J F and Troe J 2007 *J. Chem. Phys.* **127** 244305.
[4] Christophorou L G and Olthoff J K 2004 *Fundamental Electron Interactions with Plasma Processing Gases* (New York: Kluwer Academic/Plenum).
[5] Christophorou L G and Olthoff J K 2000 *J. Phys. Chem. Ref. Data* **29** 267-327.
[6] Klots C E 1976 *Chem. Phys. Lett.* **38** 61-64.
[7] Hotop H, Ruf M-W, Allan M and Fabrikant I I 2003 *Adv. At. Mol. Opt. Phys.* **49** 85-216.
[8] Dashevskaya E I, Litvin I, Nikitin E E and Troe J (in press) *Phys. Chem. Chem. Phys.*
[9] Braun M, Barsotti S, Marienfeld S, Leber E, Weber J M, Ruf M-W and Hotop H 2005 *Eur. Phys. J. D* **35** 177-191.
[10] Crompton R W and Haddad G N 1983 *Aust. J. Phys.* **36** 15-25.
[11] Petrovic Z L and Crompton R W 1985 *J. Phys. B* **17** 2777-2791.
[12] LeGarrec J L, Sidko O, Queffelec J L, Hamon S, Mitchell B A and Rowe B R 1997 *J. Chem. Phys.* **107,** 54-63.

[13] Goulay F, Rebrion-Rowe C, Carles S, Le Garrec J L and Rowe B R 2004 *J. Chem. Phys.* **121,** 1303-1308.
[14] Christophorou L G and Datskos P G 1995 *Int. J. Mass Spectrom. Ion Processes* **149/150** 59-77 (1995).
[15] Foster M S and Beauchamp J L 1975 *Chem Phys. Lett.* **31** 482-486.
[16] Fernandez A I, Viggiano A A, Miller T M, Williams S, Dotan I, Seeley J V and Troe J 2004 *J. Phys. Chem. A* **108** 9652-9659.
[17] Dunbar R C, (personal communications).
[18] Fehsenfeld F C 1970 *J. Chem. Phys.* **53** 2000-2004.
[19] Rains L J, Moore H W and McIver R T 1978 *J. Chem. Phys.* **68** 3309-3311.
[20] Španěl P, Matejcik S and Smith D 1995 *J. Phys. B* **28** 2941-2957.
[21] Chen C L and Chantry P J 1979 *J. Chem. Phys.* **71** 3897-3907.
[22] Ferguson E E 1972 in *Ion-Molecule Reactions*, vol. 2, Ed. J. L. Franklin (London: Butterworth), chap. 8, p. 370.
[23] Hickam W M and Berg D 1958 *J. Chem. Phys.* **29** 517-523.
[24] Smith D, Španěl P, Matejcik S, Stamatovic A, Märk T D, Jaffke T and Illenberger E 1995 *Chem. Phys. Lett.* **240** 481-488.
[25] Braun M, Marienfeld S, Ruf M-W and Hotop H (to be published).
[26] Champion R L, Dyakov I V, Peko B L and Wang Y 2001 *J. Chem. Phys.* **115** 1765-1768.
[27] Miller T M, Arnold S T and Viggiano A A 2003 *Int. J. Mass Spectrom.* **227** 413-420.
[28] Lobring K C, Check C E, Gilbert T M and Sunderlin L S 2003 *Int. J. Mass Spectrom.* **227** 361-372.
[29] Bopp J C, Roscioli J R, Johnson M A, Miller T M, Viggiano A A, Villano S M, Wren S W and Lineberger W C 2007 *J. Chem. Phys.* **111** 1214-1221.
[30] Grimsrud E P, Chowdhury S and Kebarle P 1985 *J. Chem. Phys.* **83** 1059-1068.
[31] Chen E C M and Chen E S 2004 *J. Chromatography A* **1037** 83-106.
[32] Ervin K M, Anusiewicz W, Skurski P, Simons J and Lineberger W C 2003 *J. Phys. Chem. A* **107** 8521-8529.
[33] Miller T M, Friedman J F and Viggiano A A 2004 *J. Chem. Phys.* **120** 7024-7028.
[34] Miller T M 2005 *Adv. At. Mol. Opt. Phys.* **51** 299-342.
[35] Le Garrec J-L, Steinhurst D A and Smith M A 2001 *J. Chem. Phys.* **114** 8831-8835.
[36] Liu Y, Suess L and Dunning F B 2005 *J. Chem. Phys.* **122** 214313.
[37] Tsang W and Herron J T 1992 *J. Chem. Phys.* **96** 4272-4282.
[38] Van Doren J M, Miller T M, Viggiano A A, Španěl P, Smith D, Bopp J C and Troe J (in press) *J. Chem. Phys.*
[39] Borrelli R 2007 *Chem. Phys. Lett.* **445** 84-88.